


Hydrophobic and Hydrophilic Effects on Water Structuring and Adhesion in Denture Adhesives

Simrone K Gill,¹ Nima Roohpour,² Yiran An,³ Julien E Gautrot,³ Paul D Topham,^{4}  Brian J Tighe¹*

1. Biomaterial Research Unit, School of Engineering and Applied Science, Aston University, Birmingham B4 7ET, UK.
2. Consumer Healthcare R&D, GlaxoSmithKline, St George's Avenue, Weybridge, Surrey, KT13 ODE, UK.
3. School of Engineering and Materials Science, Queen Mary University of London, Mile End Road, London, E1 4NS, UK.
4. Aston Institute of Materials Research, School of Engineering and Applied Science, Aston University, Birmingham, B4 7ET, UK.

This article has been accepted for publication and undergone full peer review but has not been through the copyediting, typesetting, pagination and proofreading process which may lead to differences between this version and the Version of Record. Please cite this article as an 'Accepted Article', doi: 10.1002/jbm.a.36341

ABSTRACT

Denture adhesives are designed to be moisture-sensitive through the inclusion of a blend of polymer salts with varying degrees of water-sensitivity. This enables the adhesive to mix with saliva *in vivo* and activate its high tack, through the formation of a mucilaginous layer. We report for the first time, the use of differential scanning calorimetry (DSC) to study a series of hydrophobic and hydrophilic polymeric systems in order to correlate water-structuring behavior with adhesion strength. Adhesive bonding of the more hydrophobic variants was higher than that of a commercial-based control and a more hydrophilic polymer system in both lap shear and tensile configurations. Water-binding data suggested that increasing the hydrophobicity of the maleic acid copolymer substituents led to decreased levels of freezing water. In comparison, increasing the hydrophilic nature of the polymer backbone gave higher levels of freezing water within the hydrated samples. The results of this study emphasize the importance of varying the levels of hydrophobic and hydrophilic components within denture adhesive formulations, alongside the types of water present within the adhesive systems. This phenomenon has shown the potential to fine-tune the adhesive properties and failure mode against poly(methyl methacrylate), PMMA, surfaces.

KEYWORDS: polymers, adhesives, prosthodontics, water-structuring, differential scanning calorimetry.

INTRODUCTION

The popularity and use of denture adhesives has increased over the years and such commercial products play an important role in prosthetic dentistry [1, 2] as they improve the fit, comfort, chewing ability and performance of dentures [3-6]. Denture adhesives are required to form temporary adhesive bonds between the denture, typically fabricated from poly(methyl methacrylate) (PMMA), [7] and the denture-bearing oral mucosa [2, 8]. An adhesive failure from the tissue interface is the preferred failure outcome [9-11] when the patient removes the denture at the end of the day, in order to avoid the unpleasant feeling of residue left on the oral tissue [1, 2, 12-14]. The failure mode is dictated by the balance between adhesive and cohesive strength. When the locus of failure occurs at an interface, this is referred to as adhesive failure. Conversely, a cohesive failure occurs in the bulk of the adhesive [15].

Denture adhesives exist in a number of forms; powders, pastes, strips, cushions or pads [3, 16]. This study focuses on the most commonly used “paste form” [16]. Most formulation strategies have evolved to take advantage of the humid environment within the oral cavity by mixing with saliva, which hydrates the adhesive, and produces a mucilaginous layer with high tack and adherent properties [17]. Current commercial formulations are typically based on a combination of synthetic and naturally-based salts of polymers, such as poly(methylvinylether-maleic acid) (PMVE-MA) and sodium carboxymethylcellulose (NaCMC) [16, 18, 19]. These components contain so-called “active” hydrophilic groups that enable the adhesives to swell in the presence of saliva, yet the structural role particularly that played by the

alternating PMVE-MA copolymer, is not yet well understood. Petrolatum and mineral oil are also added to the adhesive pastes, as hydrocarbon carriers to disperse the active components and function as thinning and binding agents [20, 21].

In this work, a control formulation based on commercial non-zinc-containing denture adhesive compositions [22-24] was used as a benchmark. Additionally, batches whereby the methylvinylether group (OCH₃) of the PMVE-MA constituent was substituted by either more hydrophilic or hydrophobic groups were also included, as illustrated in Figure 1.

Differential Scanning Calorimetry (DSC) is a technique that allows the amount of *so-called* 'freezing water' to be calculated. Freezing water is water that does not interact with the polymer and maintains the tetrahedral ice-like structure of water, showing similar thermal phase transitions to bulk water (*i.e.* melts at 0 °C) [25, 26]. Water that is bound to the polymer does not freeze and therefore the amount of unbound (freezing) water can be calculated from the DSC thermogram (see the Materials & Methods section for further details).

The objectives of this study were to correlate the levels of freezing water, which has not yet been considered, to the adhesive performance of hydrated denture adhesives as a function of hydrophobicity levels (illustrated in Figure 2).

MATERIALS & METHODS

Materials

Poly(methylvinylether-maleic acid) (PMVE-MA), (Gantrez MS-955) and sodium carboxymethylcellulose (NaCMC) were purchased from Ashland, USA. Petrolatum and mineral oil were purchased from Sonneborn, USA.

Accepted Article
Butylvinylether (BVE), maleic anhydride (MAn) and poly(acrylic acid-maleic acid) (PAA-MA) were purchased from Sigma-Aldrich. Poly(styrene-maleic anhydride) (PS-MAn) was purchased from Polysciences, Inc. Benzoyl peroxide (BPO) was purchased from BDH Ltd and toluene, ethyl acetate and methanol were purchased from Fischer Scientific. PMMA substrates for lap shear adhesion testing were provided by GlaxoSmithKline (Weybridge, UK) with dimensions of 2.3 x 7.5 x 0.3 cm. Melinex® (polyethylene terephthalate, PET) was purchased from PSG Group Ltd and cut to the same dimensions as the PMMA substrates. All reagents were used as obtained without further purification.

**Free radical polymerization of poly(butylvinylether-maleic anhydride),
PBVE-MAn**

The following method describes the polymerization of PBVE-MAn at 1:1 monomer feed molar ratio. 40 mL of toluene, 10 mL of ethyl acetate, BPO initiator (40 mg) and MAn (2 g) were added to a 250 mL three-neck round bottom flask equipped with a reflux condenser, thermometer, nitrogen gas inlet system and a magnetic stirrer bar. The flask was sealed with a rubber septum and the mixture was purged with nitrogen at 70 °C via a syringe and needle. After 15 minutes, liquid BVE monomer (2.6 mL) was added to the reaction mixture (via a syringe and needle) and left to copolymerize for 6 hours. The polymerization product was isolated by vacuum filtration and washed three times with methanol. The final polymer product was then filtered and dried under vacuum at room temperature. The characterization methods used for the polymer synthesized are provided in the Supporting Material.

Hydrolysis of PBVE-MAn and PS-MAn to poly(butylvinylether-maleic acid), PBVE-MA and poly(styrene-maleic acid), PS-MA

The maleic anhydride component of the polymer products was hydrolyzed in DI water (from the Purite Select system) at 80 °C, with the progressive addition of 1 M NaOH until pH 11 was reached. Subsequently, the resulting solutions were freeze-dried, using a VirTis BenchTop freeze dryer to give powders as the final products.

Adhesive formulations

The control formulation was made according to published patents [27, 28] and compositions of non-zinc-containing commercial formulations [22-24]. Firstly, 29 g of petrolatum was mixed with 17 g of mineral oil using a speed mixer, Synergy device DAC 400.1 fvz for 2 minutes (2700 rpm). 30 g of PMVE-MA calcium/sodium partial salts and 24 g of NaCMC were then added and mixed again for 2 minutes (2700 rpm). The formulation was then coarsely mixed with a spatula in order to allow any excess powder to be dispersed within the mixture before mixing again for 4 minutes (2700 rpm). For the variant formulations, batches were made by replacing either 25 % or 50 % of the PMVE-MA calcium/sodium partial salts with either PAA-MA, PBVE-MA or PS-MA as shown in Figure 1.

Adhesion studies - lap shear strength

Lap shear adhesion strength of the formulations were assessed according to our previous methods [29]. The samples were mixed with DI water at a ratio of 1:1 (wt %) and placed between two clean substrates (either PMMA or PET). The overlap area in each test was 2.3 x 1.5 cm [see Figure 2(a)]. A 200 g weight was placed on top of the overlap for 5 seconds to allow constant

pressure to be exerted upon each sample. When placed in the tensometer grips, DI water (~0.18 mL) was sprayed once onto the strips before the test was conducted. Each sample was tested at room temperature, 30 (\pm 5) seconds after mixing. An Hounsfield Instron tensometer equipped with a 10 N load cell was used to conduct the lap shear adhesion measurements. The samples were pulled apart at a rate of 10 mm/min and the final adhesive strength (kPa) was obtained from the force at break (N) divided by the interfacial surface area of the hydrated adhesive (mm²), as shown in Equation 1. Six samples were measured for each adhesive variant and the average adhesion strength is reported. The error bars shown indicate \pm standard deviation.

$$\text{Adhesion strength (kPa)} = \left(\frac{\text{Max } F \text{ (N)}}{\text{surface area (mm}^2\text{)}} \right) * 1000 \quad (\text{Equation 1})$$

Tensile adhesion

The tensile adhesive strength was measured according to an adapted ISO-10873 procedure, which was modified to align with the conditions performed in the lap shear test. An Instron 3343 machine was used, alongside a pressure-sensitive shaft with a diameter of 20 mm and a PMMA sample holder (cylindrical dimension) with a diameter of 22 mm and depth of 0.5 mm. The formulations were mixed with DI water at a ratio of 1:1 (wt %) using a spatula before the hydrated adhesive was placed onto the centre of the sample holder. A sufficient amount of hydrated adhesive was used (ca. 0.2 g) to ensure that the surface area of the pressure sensitive shaft was fully covered without over spilling. A load of 9.8 N was applied by the pressure sensitive shaft at a cross-head speed of 5 mm/min and the load stayed in position for 30 seconds, before the pressure sensitive shaft was pulled in the

opposite direction at a cross-head speed of 10 mm/min. Six samples were measured for each adhesive variant and the average adhesion strength values are reported. The error bars shown indicate \pm standard deviation.

Water-structuring studies - differential scanning calorimetry (DSC)

Differential scanning calorimetry (DSC) was carried out using a Perkin Elmer DSC 7, equipped with a thermal analysis controller TAC 7/DX and Intracooler 2. The formulations were mixed with DI water, 1:1 (wt %) before the following temperature profile was run: cool from 20 °C to -40 °C (at a rate of 20 °C/min), cool to -50 °C (at a rate of 5 °C/min), heat to -25 °C (at a rate of 10 °C/min) and then to 20 °C (at a rate of 5 °C/min). The area under the melting endotherm peak was measured and the proportion of freezing water was calculated (expressed as a percentage of the total sample weight) using a calibration graph produced by distilled water; the heat of fusion of freezing water contained in water swollen polymers is assumed to be identical to the heat of fusion of pure water [30].

$$\Delta H (\text{sample}) = \frac{\text{area under peak}}{\text{weight of sample}} \quad (\text{Equation 2})$$

The percentage of freezing water was then obtained by:

$$\text{Freezing water (\%)} = \left(\frac{\Delta H \text{ sample}}{\Delta H \text{ of pure water}} \right) * 100 \quad (\text{Equation 3})$$

And ΔH of pure water = 333.77 J g⁻¹

This temperature program was repeated three times on three separate samples for each adhesive and results are presented as an average and the error bars shown indicate \pm standard deviation.

Tensile failure patterns - Optical microscopy

In order to get microscopic images of the tensile fibril patterns, samples were detached in a tensile configuration between PMMA plates at a rate twenty times slower compared to the tensile adhesion quantitative method explained above. This provided qualitative information on the fibril failure patterns between the variants. Two PMMA plates (dimensions of 15 mm x 6 mm x 3 mm) were bonded with hydrated adhesive samples (1:1, DI water wt %) and mounted onto a commercial microtester (Deben, 200 N tensile stage, UK). The cross section area of adhesive attachment was 3 mm x 6 mm and one of the plates was translated away from the other at a constant rate of 0.5 mm/min⁻¹ and the failure patterns were observed. Images were captured using an Olympus BX60 upright compound microscope.

Statistical analysis

SPSS software was used to carry out the statistical analysis. Data were analyzed by one-way ANOVA or two-way ANOVA in conjunction with Tukey's HSD test to evaluate the statistical significance of adhesion strength amongst the adhesive formulations and a value $p < 0.05$ was considered to be statistically significant.

RESULTS

Figure 3 shows similar trends amongst the variants in the lap shear experiments when tested against (a) PET and (b) PMMA substrates however the adhesion strength of all formulations was reduced in the PMMA/PMMA system compared to when sheared against the PET substrates. Increasing the hydrophilic character of the polymeric system (PAA-MA variants) gave significantly lower adhesive strength than the control ($p < 0.01$) whereas the hydrophobic derivatives (except for PS-MA 25% against PET and both PS-MA

loadings against PMMA, $p > 0.05$) delivered greater adhesion strength than the control ($p < 0.05$) and the hydrophilic variant, in both substrate systems.

Introducing flexible butyl groups into the polymer backbone brought about the greatest adhesive strength out of all the formulations; $9.3 (\pm 0.8)$ kPa at 50% (against PMMA) and $13.0 (\pm 0.9)$ kPa at 25% (against PET) replacement of the PMVE-MA content. The PS-MA containing systems did not enhance adhesion to the same extent as the PBVE-MA variants. Both hydrophobic adhesives gave cohesive failures whilst the control and more hydrophilic systems gave adhesive failures, independent of the substrates used.

Clear trends are shown in the DSC data [Fig. 4 (a)]; increasing the hydrophilic nature of the formulation gave increased levels of freezing water ($\sim 8\%$ higher for PAA-MA at 50 %) compared to the control ($p < 0.01$). Conversely, when the hydrophobicity of the formulation was increased, lower levels of freezing water ($\sim 4\%$ for PBVE-MA and $\sim 7\%$ lower for PS-MA at 50 %, $p < 0.01$) were observed compared to the control [$33.5 (\pm 1.1)\%$].

Figure 5 (a) shows the tensile adhesion strength values of the hydrated formulations between PMMA substrates. Complimentary to the primary adhesion quantifying technique used in this work (shear testing), formulations of 50 % incorporation of the hydrophilic and hydrophobic variants were used. Average adhesion values followed the order PBVE-MA > PSMA > PMVE-MA > PAA-MA in exact agreement with the lap shear adhesive strength trends. However, only the PBVE-MA variant gave statistical significance ($p < 0.05$) from the control. There was no statistical significance between the hydrophobic variants ($p > 0.05$), however both gave significantly higher

adhesion compared to the hydrophilic variant ($p < 0.01$). The values for the tensile adhesion strength were considerably higher but gave larger standard deviations compared to the shear setup, as expected [31, 32]. The loci of failure were also the same as observed in the shear experiments with the exception of the control, which gave cohesive failures in the tensile studies.

Figure 5 (b) shows the fibril profiles (captured by optical microscope) produced when the hydrated adhesives were subjected to a tensile detachment process, at a considerably slower rate to the experiment in Figure 5 (a). The control and the more hydrophilic adhesives behaved similarly; both resulting in adhesive failures and producing thin fibrils. On the other hand, the hydrophobically-modified adhesives gave cohesive failures with the PBVE-MA samples producing thicker fibrils, whilst the PS-MA derivative produced aggregated regions between thin fibrils.

DISCUSSION

Denture adhesives rely heavily on the physico-chemical interactions after mixing with saliva for optimum performance. A systematic approach of increasing the hydrophobicity of the maleic acid copolymer substituent was employed in this study. The overriding aim was to probe these hydrophobic effects on the distribution of the types of water once the polymeric systems were hydrated and how this phenomenon influenced adhesion.

The lap shear adhesion strength of the variant systems was assessed against either PET or PMMA substrates. PET has a similar surface energy to that of PMMA, yet the surfaces of PET show less variation (batch to batch) and are typically smoother than PMMA (as indicated by the values in Table S2 for the

surface free energy and AFM and SEM characterization of the substrates in Figures S1 and S2 in the Supporting Material). Using PET in addition to PMMA, enabled further understanding of the adhesive systems, in terms of the chemical modifications made to the PMVE-MA backbone and the resultant effects on adhesion to moderate surface energy substrates. The aim was to eliminate the surface effects that PMMA may impose on adhesive behavior.

Both substrate systems gave the same adhesive trends; the hydrophobic systems outperformed the hydrophilic systems, and produced cohesive failures against the relatively hydrophobic substrates (representing the denture base). The adhesion against the PMMA substrates was lower overall than the values reached in the PET system, even though both substrates have comparable wettability characteristics. This can be attributed to the rougher morphology of the PMMA surface [15] interfering with the adhesive performance of the samples, as the adhesives fail to make true molecular contact with the substrates.

Molecular conformability appeared to favor the PBVE-MA over the PS-MA based variants; the flexible butyl chains were less restricted and could interact with the other molecular species in the formulation and the substrates more easily compared to the sterically hindered styrene groups. Overall, in the majority of samples, increasing the loading the polymeric variants from 25 % to 50% incorporation (replacing the PMVE-MA content) did not produce a significant effect on adhesion ($p > 0.05$) with the exception of the PS-MA variants in the PET shear setup. PS-MA ($p < 0.05$) and PAA-MA ($p < 0.01$) variants gave a significant difference in freezing water levels on increasing loading content in the DSC studies.

The results in Figure 4 (a) show that the hydrophobic variants reduced the amount of freezable water in the hydrated polymeric system compared to the control; conversely the PAA-MA system gave increased freezing water levels. Higher levels of freezing water in the adhesive system led to the formation of weak boundary layers, which resulted in less interaction between the substrate and the adhesive (adhesive failures).

The presence of the hydrophobic groups, in the context of this work, function as structure-makers and force water to change (locally at the interface) from its “flickering cluster” form [Figure 6 (a)] to a more ordered state around the hydrophobic regions as illustrated in Figure 6 (b).

The hydrophobic adhesive formulations also outperformed the more hydrophilic formulation in the tensile arrangement [Figure 5 (a)] and produced cohesive failures. However, the influence of molecular conformability (butylvinylether vs styrene) in the hydrophobic systems did not impact the adhesive behavior to the same extent as observed in the lap shear adhesive strength experiments. It was important to assess the adhesive systems in both shear and tensile configurations, as both modes of deformation are experienced *in vivo* during mastication.

Optical microscopy images [Figure 5 (b)] provided an insight into the adhesive failure of the hydrated samples. These images reflect the macroscopic behavior of interactions at molecular level and confirmed that the fibril profiles are clearly influenced by chemical composition; the control and more hydrophilic adhesives both produced thin fibrils, accompanied by adhesive failures. Conversely, the more hydrophobic formulations gave cohesive failures with thicker fibrils observed in the PBVE-MA system, whilst the PS-

MA derivative produced aggregated regions in between its fibrils. The 'hydrophobic effect' forced the water to restructure which influenced the polymer and the resultant fibril formations and enhanced the adhesive capabilities of the polymers at the interface.

In conclusion, this study has demonstrated the potential to optimize the adhesion strength of conventional denture adhesives by relatively simple structural modifications to the PMVE-MA component. This was achieved by the inclusion of groups with more hydrophobic character, which consequently forced the water molecules to become more ordered around the hydrophobic domains once they were hydrated.

ACKNOWLEDGEMENTS

This work was supported by the BBSRC and GSK under the Industrial CASE Studentship Scheme (grant number – BB/L502200/1).

There are no conflicts of interest with this work.

REFERENCES

1. Coates, A. Usage of denture adhesives. *Journal of Dentistry* 2000;**28**(2):137-140.
2. Kulak, Y., M. Özcan, and A. Arıkan. Subjective assessment by patients of the efficiency of two denture adhesive pastes. *Journal of Prosthodontics* 2005;**14**(4):248-252.
3. Papadiochou, S., I. Emmanouil, and I. Papadiochos. Denture adhesives: a systematic review. *The Journal of Prosthetic Dentistry* 2015;**113**(5):391-397.
4. Coates, A. Denture adhesives: a review. *Australian Prosthodontic Journal/Australian Prosthodontic Society* 1994;**9**:27-31.
5. Grasso, J.E. Denture adhesives: changing attitudes. *The Journal of the American Dental Association* 1996;**127**(1):90-96.
6. Rendell, J.K., T. Gay, J.E. Grasso, R.A. Baker, and J.L. Winston. The effect of denture adhesive on mandibular movement during chewing. *The Journal of the American Dental Association* 2000;**131**(7):981-986.
7. John, J., S.A. Gangadhar, and I. Shah. Flexural strength of heat-polymerized polymethyl methacrylate denture resin reinforced with glass, aramid, or nylon fibers. *The Journal of Prosthetic Dentistry* 2001;**86**(4):424-427.

8. Guo, X., F. Deng, L. Li, and R.K. Prud'homme. Synthesis of biocompatible polymeric hydrogels with tunable adhesion to both hydrophobic and hydrophilic surfaces. *Biomacromolecules* 2008;**9**(6):1637-1642.
9. Grasso, J.E., J. Rendell, and T. Gay. Effect of denture adhesive on the retention and stability of mixillary dentures. *The Journal of prosthetic dentistry* 1994;**72**(4):399-405.
10. Psillakis, J.J., R.F. Wright, J.T. Grbic, and I.B. Lamster. In practice evaluation of a denture adhesive using a gnathometer. *Journal of Prosthodontics* 2004;**13**(4):244-250.
11. Ahmad, M. and K.H. Kamarudin. Masticatory efficacy and bite force in complete dentures: a study of denture adhesive. *Hong Kong Dent J* 2010;**7**:67-73.
12. Sato, Y., Y. Kaiba, and I. Hayakawa. The evaluation of denture retention and ease of removal from oral mucosa on a new gel-type denture adhesive. *Nihon Hotetsu Shika Gakkai Zasshi* 2008;**52**(2):175-182.
13. Adisman, I.K. The use of denture adhesive as an aid to denture treatment. *The Journal of Prosthetic Dentistry* 1989;**62**(6):711-715.
14. Hong, G., T. Maeda, and T. Hamada. The effect of denture adhesive on bite force until denture dislodgement using a gnathometer. *Int Chin J Dent* 2010;**10**:41-45.
15. Fang, J., C. Wang, Y. Li, Z. Zhao, and L. Mei. Comparison of bacterial adhesion to dental materials of polyethylene terephthalate (PET) and polymethyl methacrylate (PMMA) using atomic force microscopy and scanning electron microscopy. *Scanning* 2016;
16. da Rosa, W.L.d.O., S.G.D. de Oliveira, C.H. Rosa, A.F. da Silva, R.G. Lund, and E. Piva. Current trends and future perspectives in the development of denture adhesives: an overview based on technological monitoring process and systematic review. *Journal of Biomedical Sciences* 2015;**4**(1):1-7.
17. Chang, T.-S. and D. DiFerdinando, Highly crosslinked lower alkyl ether/maleic anhydride copolymer. 1997, Google Patents.
18. Han, J.-m., G. Hong, K. Hayashida, T. Maeda, H. Murata, and K. Sasaki. Influence of composition on the adhesive strength and initial viscosity of denture adhesives. *Dental Materials Journal* 2014;**33**(1):98-103.
19. Tazi, M., Y.T. Kwak, B. Gangadharan, and R.K. Haldar, Denture adhesive. 1991, US 5,037,924.
20. Desmarais, A.J., Denture adhesive composition. 1991, US 5024701 A.
21. Tian, T., W. Zhu, and S. Yu. Preparation and lab evaluation of a new denture adhesive. *Journal of Wuhan University of Technology-Mater. Sci. Ed.* 2011;**26**(6):1036-1040.
22. Tezvergil-Mutluay, A., R.M. Carvalho, and D.H. Pashley. Hyperzincemia from ingestion of denture adhesives. *The Journal of prosthetic dentistry* 2010;**103**(6):380-383.
23. Munoz, C.A., L. Gendreau, G. Shanga, T. Magnuszewski, P. Fernandez, and J. Durocher. A Clinical Study to Evaluate Denture Adhesive Use in Well-Fitting Dentures. *Journal of Prosthodontics* 2012;**21**(2):123-129.

24. Kore, D.R., M.T. Kattadiyil, D.B. Hall, and K. Bahjri. In vitro comparison of the tensile bond strength of denture adhesives on denture bases. *The Journal of Prosthetic Dentistry* 2013;**110**(6):488-493.
25. Higuchi, A., J. Komiyama, and T. Iijima. The states of water in gel cellophane membranes. *Polymer Bulletin* 1984;**11**(2):203-208.
26. Hodge, R., G.H. Edward, and G.P. Simon. Water absorption and states of water in semicrystalline poly (vinyl alcohol) films. *Polymer* 1996;**37**(8):1371-1376.
27. Chang, T.-S., L.J. Zientek, A. Viningauz, and M.L. Scheps, Denture fixative composition. 1983, US 4,373,036.
28. Wong, E., H.C. Clarke, R.C. Gasman, J.D. Synodis, and A.J. Smetana, Denture adhesive compositions comprising a polymeric activator. 2002, US 6,423,762 B1.
29. Gill, S.K., N. Roohpour, P.D. Topham, and B.J. Tighe. Tuneable Denture Adhesives using Biomimetic Principles for Enhanced Tissue Adhesion in Moist Environments. *Acta Biomaterialia* 2017;**63**:326-335.
30. Pedley, D.G. and B.J. Tighe. Water binding properties of hydrogel polymers for reverse osmosis and related applications. *Polymer International* 1979;**11**(3):130-136.
31. Pocius, A., *Adhesion and Adhesives Technology, An introduction: The chemistry and physical properties of elastomer-based adhesives*. 2002, Hansen Gardner Publications, Inc., Maplewood.
32. Matos-Pérez, C.R., J.D. White, and J.J. Wilker. Polymer composition and substrate influences on the adhesive bonding of a biomimetic, cross-linking polymer. *Journal of the American Chemical Society* 2012;**134**(22):9498-9505.
33. Nelson, D.L., A.L. Lehninger, and M.M. Cox, *Lehninger principles of biochemistry*. 2008 Macmillan.

LEGENDS

Figure 1. Adhesive formulation components by weight percentage and the chemical structures of the polymeric variants used in this study.

Figure 2. Overall experimental strategy employed in this work; (a) lap shear and (b) tensile bond setup to assess the adhesive strength of hydrated denture adhesive formulations and (c) differential scanning calorimetry (DSC) setup used to assess the levels of freezing water within hydrated adhesive formulations.

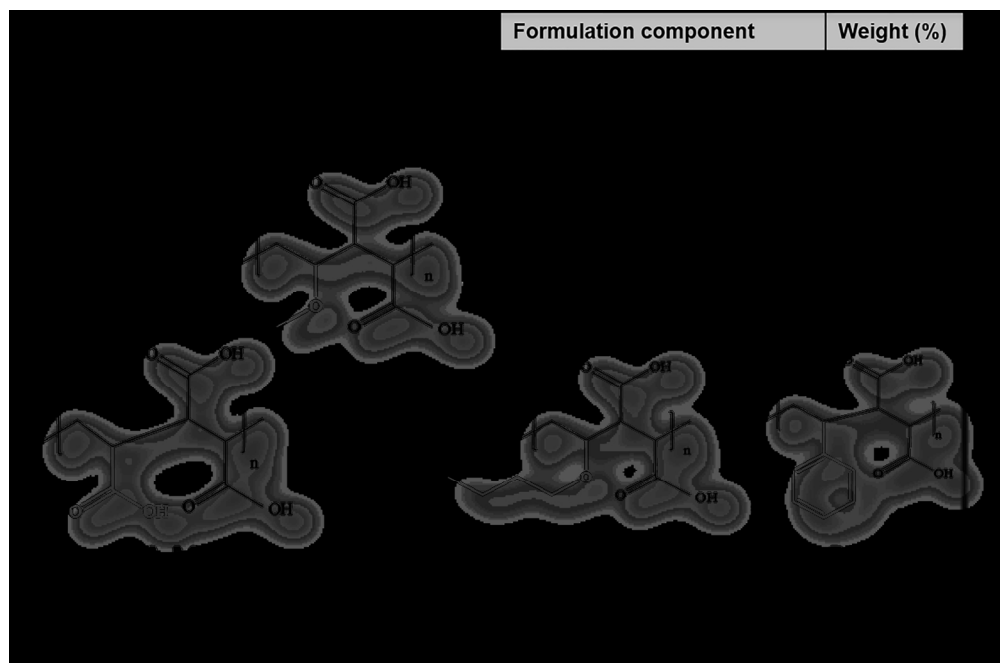
Figure 3. Maximum lap-shear adhesion strength of hydrated adhesive samples against (a) PET substrates and (b) PMMA substrates as a function of

the polymeric variant. The asterisk (*) is used to identify data that have a p value of < 0.05 , and show statistically significant differences from the control. Variants identified with the same letter are not significantly different from each other ($p > 0.05$). Representative primary force-extension curves obtained during the lap shear experiments of the hydrated adhesives, each at 50% replacement of PMVE-MA content with the copolymer against (c) PET and (d) PMMA substrates.

Figure 4 (a) The freezing water levels of hydrated adhesive samples, calculated by DSC and (b) representative endothermic peaks obtained during the DSC studies of the hydrated adhesives. The asterisk (*) is used to identify data that have a p value of < 0.05 , and show statistically significant differences from the control. Variants identified with the same letter are not significantly different from each other ($p > 0.05$).

Figure 5. (a) Maximum tensile adhesion strength of hydrated adhesive samples against PMMA substrates as a function of the polymeric variant. The asterisk (*) is used to identify data that have a p value of < 0.05 , and show statistically significant differences from the control. Variants with the same letter are not significantly different from each other ($p > 0.05$). (b) Optical microscopy images of the tensile failure patterns of the hydrated formulations between PMMA plates.

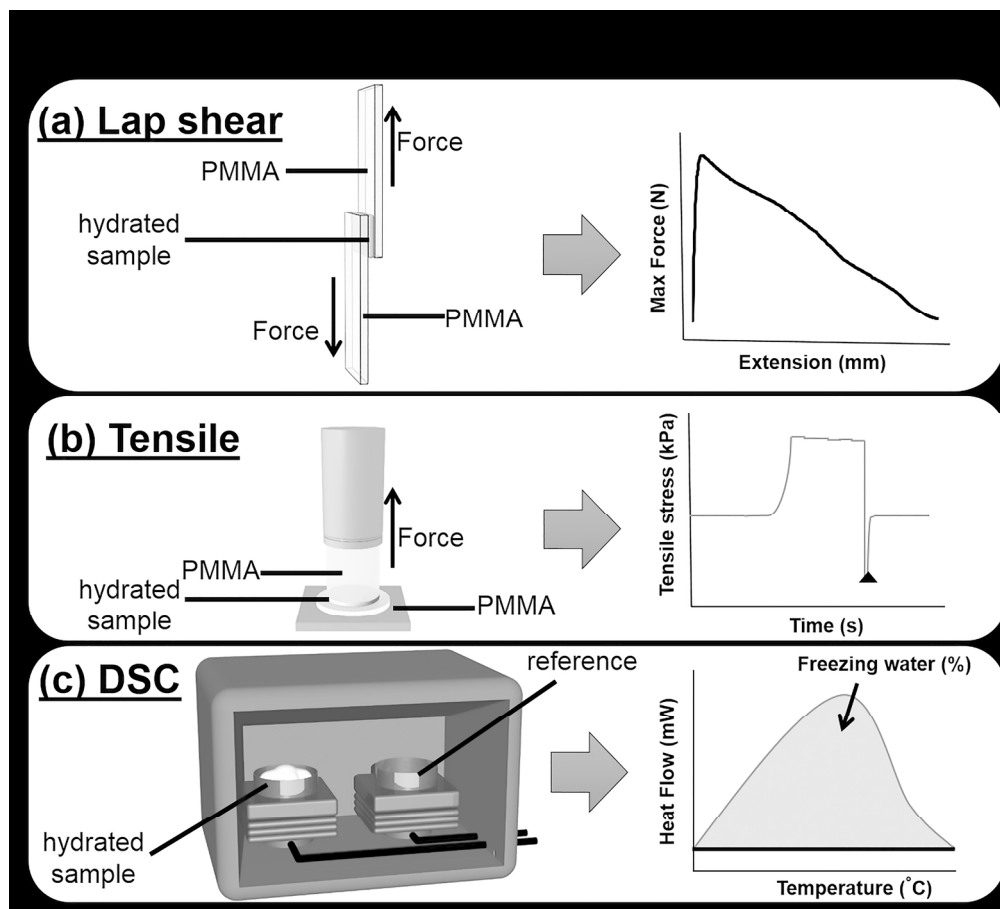
Figure 6. Schematic representation of the arrangement of (a) water molecules in the “bulk” phase (“freezable” water) and (b) around a hydrophobic hydrocarbon chain (here butylvinylether repeat unit is shown). Adapted in part from [33].



Adhesive formulation components by weight percentage and the chemical structures of the polymeric variants used in this study.

132x86mm (300 x 300 DPI)

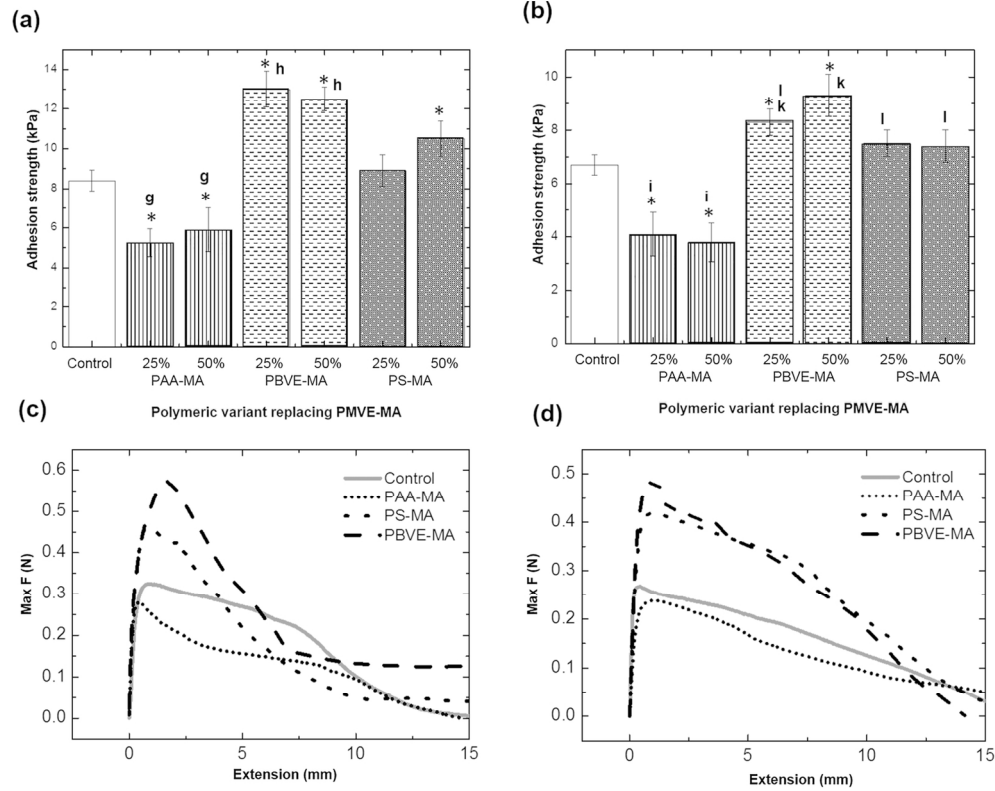
Accept



Overall experimental strategy employed in this work; (a) lap shear and (b) tensile bond setup to assess the adhesive strength of hydrated denture adhesive formulations and (c) differential scanning calorimetry (DSC) setup used to assess the levels of freezing water within hydrated adhesive formulations.

194x175mm (300 x 300 DPI)

Acce



137x108mm (300 x 300 DPI)

Accep

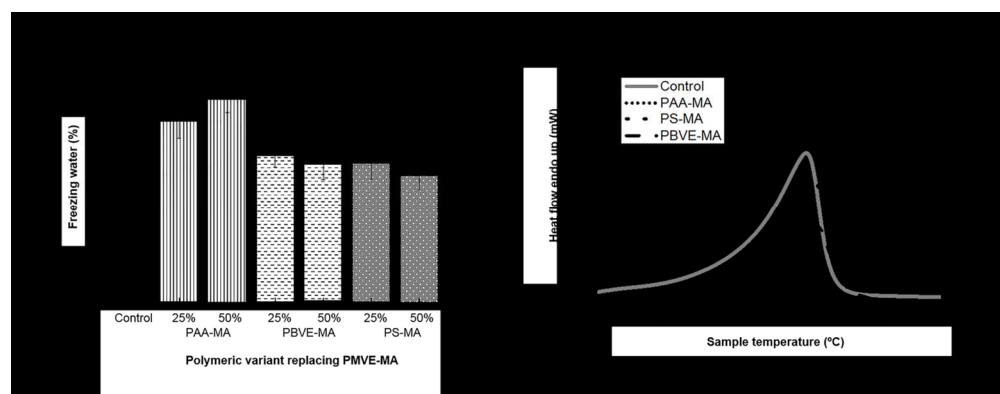
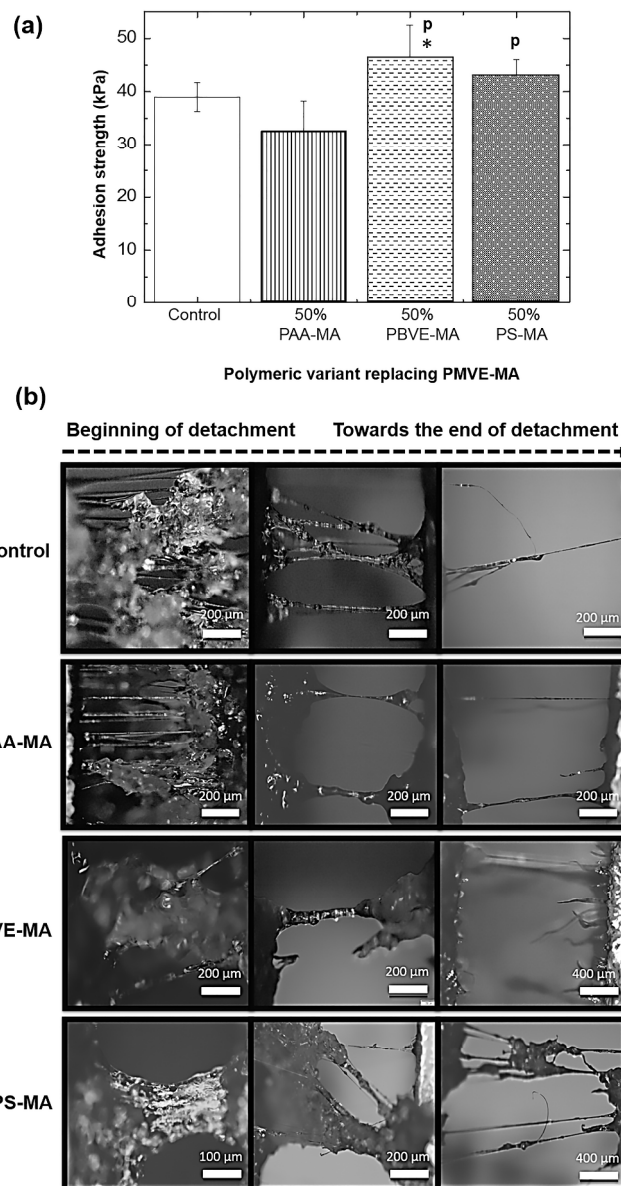


Figure 4 (a) The freezing water levels of hydrated adhesive samples, calculated by DSC and (b) representative endothermic peaks obtained during the DSC studies of the hydrated adhesives. The asterisk (*) is used to identify data that have a p value of < 0.05, and show statistically significant differences from the control. Variants identified with the same letter are not significantly different from each other ($p > 0.05$).

122x47mm (300 x 300 DPI)

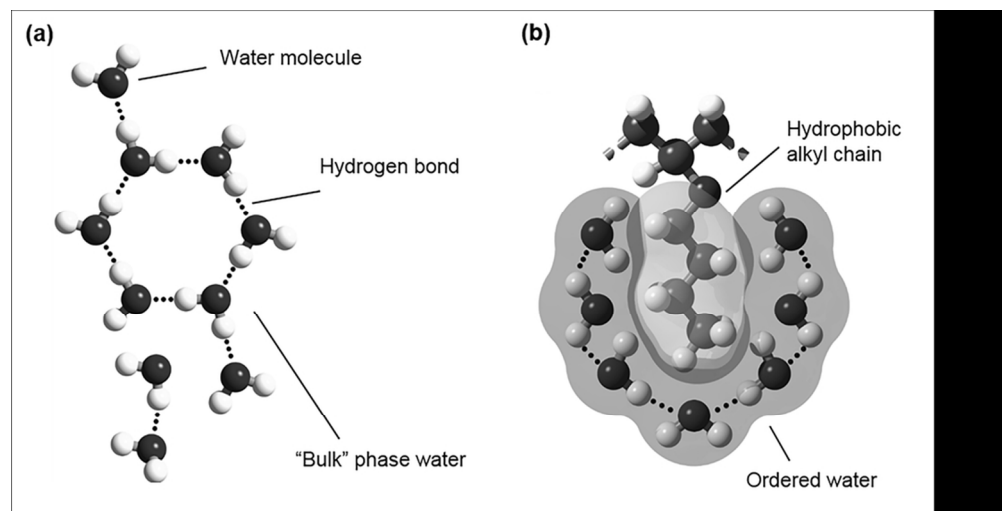
Accepted



(a) Maximum tensile adhesion strength of hydrated adhesive samples against PMMA substrates as a function of the polymeric variant. The asterisk (*) is used to identify data that have a p value of < 0.05 , and show statistically significant differences from the control. Variants with the same letter are not significantly different from each other ($p > 0.05$). (b) Optical microscopy images of the tensile failure patterns of the hydrated formulations between PMMA plates.

310x548mm (300 x 300 DPI)

A



Schematic representation of the arrangement of (a) water molecules in the "bulk" phase ("freezable" water) and (b) around a hydrophobic hydrocarbon chain (here butylvinylether repeat unit is shown). Adapted in part from [35].

91x46mm (300 x 300 DPI)

Accepted